Y and L, with regard to platinization on the external surface, can probably be attributed to the connectivity of the large cages in the two structures. In the zeolite Y structure, each supercage has four nearest neighbors and molecular diffusion can occur freely in three dimensions. In zeolite L, however, the large cavities are linearly interconnected to from one-dimensional tunnels; diffusion of large molecules such as Pt(acac)$_2$ is likely to be severely restricted. Hence it is possible with the L structure to wash the complex completely off the external surface and to dry the zeolite before substantial diffusion out of the bulk and onto the external surface can occur. The chemical tests outlined above are inexpensive and sensitive and may be of general utility in locating noble-metal catalysts in/on zeolites.

Acknowledgment. We thank Dr. Michael Schmerling, Department of Mechanical Engineering, The University of Texas at Austin, for carrying out the SEM measurements. This work was supported by a grant from the Gas Research Institute.

Registry No. Pt, 7440-06-4; Pt(acac)$_2$, 15170-57-7; MV^{2+}·2Cl$^-$, 1910-42-5; Fe(CN)$_6^{3-}$, 13408-62-3.

---

(16) Meier, W. M.; Olson, D. H. *Atlas of Zeolite Structure Types*; Juris Druck + Verlag AG: Zurich, 1978; pp 37, 59.

Contribution from the Departments of Chemistry,
Texas A&M University, College Station, Texas 77843,
and University of Delaware, Newark, Delaware 19716

Insertion Reactions of Carbon Dioxide with Square-Planar Rhodium Alkyl and Aryl Complexes

Donald J. Darensbourg,*[1a] Georg Grötsch,[1a] Philip Wiegreffe,[1a] and Arnold L. Rheingold[1b]

Received April 24, 1987

Mechanistic aspects of carbon–carbon bond forming reactions resulting from the insertion of carbon dioxide into metal–carbon bonds have been the focus of our recent attention (eq 1).[2] The

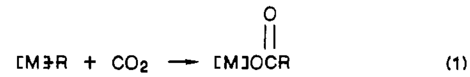

$$[\mathrm{M}]{-}\mathrm{R} + \mathrm{CO_2} \longrightarrow [\mathrm{M}]\mathrm{O}\overset{\mathrm{O}}{\overset{\|}{\mathrm{C}}}\mathrm{R} \qquad (1)$$

importance of reaction 1 stems from the fact that it constitutes a fundamental step in the use of carbon dioxide as a feedstock for organic chemicals.[3]

Comparative studies between carbonylation and carboxylation reactions based on investigations involving group 6 metal carbonyl alkyl and aryl derivatives of the type RM(CO)$_5^-$ (M = Cr, W) have been completed.[4] It was found that the two processes differ markedly with respect to several reaction variables. For carboxylation reactions a concerted process involving a transition state as shown in A was proposed on the basis of the following observations: (i) the reaction is first order in both CO$_2$ and metal substrate, (ii) activation parameters are indicative of an I$_a$ mechanism involving a great deal of bond making in the transition state, (iii) CO$_2$ insertion into the W–C bond was not retarded by excess CO (that is, the process does not involve a coordinatively unsaturated intermediate), (iv) upon increasing the nucleophilicity of the metal center, the rate of carboxylation is enhanced, and (v) the configuration at the alkyl carbon center is retained.[5]

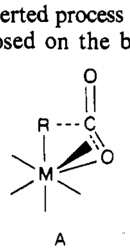

A

This report contains further observations on the insertion reactions of CO$_2$ into the Rh–C bond of several Rh(I) complexes in an attempt to better define the reaction parameters for these processes. Specifically, studies have centered on square-planar complexes of rhodium of the general formula (R$_3$P)$_3$RhR′, where R and R′ = alkyl or aryl groups. Two primary reasons for investigating reaction 2 mechanistically are (a) these species represent the best cases for possibly observing CO$_2$ coordination to the metal center prior to carbon–carbon bond formation and (b) square-planar complexes are of increasing importance in stoichiometric and catalytic synthesis of organic chemicals.[6]

$$(\mathrm{R_3P})_3\mathrm{RhR'} + \mathrm{CO_2} \rightarrow (\mathrm{R_3P})_3\mathrm{RhO_2CR'} \qquad (2)$$

Experimental Section

All manipulations were carried out either in an argon drybox or on a double-manifold Schlenk vacuum line, using freshly distilled solvents. Reagent grade benzene, toluene, and hexane were purified by distillation under nitrogen from sodium benzophenone ketyl. Me$_3$P was purchased from Strem Chemicals, Inc. (Newburgport, MA 01950). (Ph$_3$P)$_3$Rh–Ph,[7] (Ph$_3$P)$_3$Rh–Me,[7] (Me$_3$P)$_3$Rh–Me,[8] (Ph$_3$P)$_2$(CO)Rh–Me,[9] and (Ph$_3$P)$_2$(CO)Ir–Me[10] were prepared by the methods previously described. Proton NMR spectra were recorded on a Varian EM-390 spectrometer, whereas ^{13}C and ^{31}P NMR spectra were obtained on a Varian XL-200 spectrometer. Infrared spectra were determined on Perkin-Elmer 283B and IBM FTIR/85 or FTIR/32 spectrometers. GC experiments were performed with a Perkin-Elmer Sigma 2 gas chromatograph. The high-pressure infrared measurements were carried out on the IBM FTIR/85 spectrometer using a high-pressure IR cell (CIR cell, ZnSe) provided by Barnes Analytical. the reaction was carried out in a 300-mL Parr reactor connected to the CIR cell by $^1/_{16}$-in. stainless steel tubing. The sample was delivered directly from the reactor to the cell with both maintained at the pressure of the reactor. Background spectra were determined in a completely analogous manner.

Elemental analyses were obtained by Galbraith Laboratories, Knoxville, TN.

(Benzoato)tris(triphenylphosphine)rhodium(I) (2). A 0.2910-g (0.3010-mmol) amount of (Ph$_3$P)$_3$Rh–Ph (**1**) in 3 mL of benzene was reacted with CO$_2$ at a pressure of 300 psi for 24 h. Evaporation of the solvent afforded orange-red, microcrystalline **2**: yield 0.3159 g (98%); IR (C$_6$H$_6$) ν(OC)$_{as}$ 1608 (m), 1571 (m), ν(OCO)$_s$ 1354 (s), ν(C–C$_{ar}$) 1585 (w), 1500 (w), 1465 (w), 1435 (vs) cm^{-1}.

Tris(trimethylphosphine)phenylrhodium(I) (4). To a suspension of 0.3100 g (0.7003 mmol) of [(Me$_3$P)$_4$Rh]Cl (**3**) in 35 mL of toluene was added at −60 °C 0.0706 g (0.8404 mmol) of PhLi dissolved in ether/hexane. Upon slow warming to 0 °C, formation of **4** was indicated by the solvation of **3**. After 1 h of stirring at 0 °C to complete the production of **3**, the reaction mixture was filtered through Celite. After removal of the solvent at 0 °C, the resulting orange solid was redissolved in 10 mL of hexane, the solution filtered again through Celite, and the solvent evaporated until crystallization started. Following a brief warming to 40 °C, the clear solution was slowly cooled to −11 °C. After 4 days at −11 °C, orange crystals were obtained and isolated by filtration: yield 0.2100 g (74%); ^{1}H NMR (C$_6$D$_6$) δ 7.93 (m, 2 H, C$_6$H$_5$), 7.22 (m, 3 H, C$_6$H$_5$), 1.17 (m, 9 H, H$_3$CP), 1.03 (m, 18 H, H$_3$CP); ^{13}C{^{1}H} NMR

---

(1) (a) Texas A&M University. (b) University of Delaware.

(2) (a) Darensbourg, D. J.; Rokicki, A. *J. Am. Chem. Soc.* **1982**, *104*, 349. (b) Darensbourg, D. J.; Kudaroski, R. *J. Am. Chem. Soc.* **1984**, *106*, 3672.

(3) (a) Eisenberg, R.; Hendriksen, D. E. *Adv. Catal.* **1979**, *28*, 79. (b) Sneeden, R. P. A. In *Comprehensive Organometallic Chemistry*; Wilkinson, G., Stone, F. G. A., Abel, E. W., Eds.; Pergamon: Oxford, U.K., 1982; Vol. 8, p 225. (c) Ito, T.; Yamamoto, A. *Organic and Bio-Organic Chemistry of Carbon Dioxide*; Inoue, S., Yamazaki, N., Eds.; Kodonsha: Tokyo, Japan, 1982; p 79. (d) Darensbourg, D. J.; Kudaroski, R. *Adv. Organomet. Chem.* **1983**, *22*, 129.

(4) Darensbourg, D. J.; Hanckel, R. K.; Bauch, C. G.; Pala, M.; Simmons, D.; White, J. N. *J. Am. Chem. Soc.* **1985**, *107*, 7463.

(5) Darensbourg, D. J.: Grötsch, G. *J. Am. Chem. Soc.* **1985**, *107*, 7473.

(6) (a) See Chapter 3 in ref 3c and references contained therein. (b) Carmona, E.; Palma, P.; Paneque, M.; Poveda, M. L. *J. Am. Chem. Soc.* **1986**, *108*, 6424. (c) Fujiwara, Y.; Kawata, I.; Sugimoto, H.; Taniguchi, H. *J. Organomet. Chem.* **1983**, *256*, C35. (d) Fujiwara, Y.; Kawauchi, T.; Taniguchi, H. *J. Chem. Soc., Chem. Commun.* **1980**, 220. (e) Sugimoto, H.; Kawata, I.; Taniguchi, H.; Fujiwara, Y. *J. Organomet. Chem.* **1984**, *266*, C44.

(7) Keim, W. *J. Organomet. Chem.* **1968**, *14*, 179.

(8) Jones, R. A.; Mayor Real, F.; Wilkinson, G.; Galas, A. M. R.; Hursthouse, M. B. *J. Chem. Soc., Dalton Trans.* **1981**, 126.

(9) Dahlenburg, L.; Mirzaei, F.; Yardimcioglu, A. *Z. Naturforsch., B: Anorg. Chem., Org. Chem.* **1982**, *37B*, 310.

(10) Dahlenburg, L.; Nast, R. *J. Organomet. Chem.* **1974**, *71*, C49.

(THF/-d_8) δ 140.8–119.3 (m, C_6H_5) 21.7 (m, trans CH_3P), 18.4 (m, cis CH_3P); IR (C_6H_6) 1597 (w), 1588 (w), 1559 (m), 1447 (m), 1429 (m, sh), 1417 (m), 1298 (m), 1276 (m), 1197 (m), 1013 (m), 938 (vs), 848 (m), 729 (s), 702 (s) cm^{-1}. Anal. Calcd. C, 44.13; H, 7.90; P, 22.76; Rh, 25.21. Found: C, 43.88; H, 7.97; P, 22.57; Rh, 24.92.

(η^1-Benzoato)tris(trimethylphosphine)rhodium(I) (5) and (η^2-Benzoato)tris(trimethylphosphine)rhodium(I) (6). A solution of 0.4225 g (1.0349 mmol) of $(Me_3P)_3Rh$–Ph (4) in 5 mL of benzene was pressurized with 60 psi of CO_2 and stirred for 90 h while the reaction was monitored by IR spectroscopy. Initial formation of **5** was followed by conversion to **6**. A small amount of a carbonyl-containing species (ν(CO) 1946 cm^{-1}), maybe $(Me_3P)_2$(CO)Rh–OPh, was also detected. After filtration to remove a yellow, CH_3CN- and H_2O-soluble precipitate (IR bands at 1969 (m), 1825 (m), 1656 (m), 1473 (m), 1290 (w), 1265 (w), 1180 (w), 1180 (w), 1060 (s) cm^{-1}), the solvent was removed in vacuo, causing **5** to decarboxylate completely to **4**, while **6** appears to be more stable.

5: IR (C_6H_6) 1609 (m), 1431 (m), 1418 (m), 1356 (m), 1298 (m), 1276 (m), 938 (vs), 849 (m), 729 (m), 704 (m) cm^{-1}.

6: IR (C_6H_6) 1495 (m), 1448 (m), 1431 (m), 1418 (m), 1298 (m), 1276 (m), 938 (vs), 849 (m), 729 (m), 704 (m) cm^{-1}.

Reaction of 4 with CO_2 at 150-psi/High-Pressure IR Conditions. A solution of 0.3525 g (0.8634 mmol) of **4** in 30 mL of benzene was pressurized with 150 psi of CO_2 and the reaction monitored by IR spectroscopy after 30, 50, and 150 min, showing the same conversion as described above except proceeding much faster. Additionally, a considerable amount of the carbonyl-containing product (ν(CO) 1946 cm^{-1}) was observed.

Reaction of $(Ph_3P)_3Rh$–Me (7) with CO_2. A solution of 0.6645 g (0.7344 mmol) of **7** in 20 mL of benzene was pressurized with 70 psi of CO_2 for 17 h. The reaction mixture was filtered to remove a precipitate that was insoluble in benzene, acetone, and water, and the filtrate was evaporated to dryness. The resulting orange solid was redissolved in 8 mL of toluene, the solution was filtered, 20 mL of MeOH was added, and the new solution was slowly cooled to −78 °C. During this operation IR and NMR monitoring did not reveal a consistent pattern of an η^1- or η^2-acetate, whereas in the beginning of the reaction a band at 1685 cm^{-1} appeared without a corresponding absorption at 1300–1500 cm^{-1}. A small band at 1975 cm^{-1}, due to a carbonyl species, was also observed during the course of the reaction. The orange crystals were dissolved in CH_2Cl_2/CD_2Cl_2 for ^{13}C and ^{31}P NMR spectra. After removal of the chlorinated solvent, the remaining solid was redissolved in toluene, some pink precipitate separated, and the clear solution was concentrated to 5 mL, followed by addition of 20 mL of MeOH. After 4 weeks of cooling at −11 °C, $(Ph_3P)_3RhCl$[11] and $(Ph_3P)_2(CO)RhCl$[12] were isolated as crystals from a yellow oil.

(η^1-Acetato)tris(trimethylphosphine)rhodium(I) (8) and (η^2-Acetato)tris(trimethylphosphine)rhodium(I) (9). A solution of 0.3170 g (0.9163 mmol) of $(Me_3P)_3Rh$–Me was stirred under a CO_2 atmosphere (16 psi) for 7 days while the reaction was monitored by IR and NMR spectroscopy. Initial formation of **8** was observed, followed by slower generation of **9**. No CO-containing complex was detected during the reaction, but upon dissolution of a mixture of **8** and **9** in acetone a weak band at 1946 cm^{-1} was observed. In contrast to this, at 400 psi of CO_2 formation of this carbonyl compound seems to be the prominent reaction pathway; that is, **8** and **9** were not detected.

8: ^1H NMR (C_6H_6) δ 1.28 (s, 27 H, H_3CP), 1.02 (s, 3 H, H_3C); IR (C_6H_6) 1607 (m), 1425 (m), 1425 (m), 1415 (m), 1352 (m), 1298 (m), 1275 (m), 1216 (w), 1196 (m), 1008 (w), 936 (vs), 844 (m), 806 (s), 712 (m) cm^{-1}.

9: ^1H NMR (C_6H_6) δ 1.28 (s, 27 H, H_3CP), 1.07 (s, 3 H, H_3C); IR (C_6H_6) 1484 (m), 1455 (m), 1425 (m), 1415 (m), 1288 (m), 1257 (m), 1216 (w), 1196 (m), 1008 (w), 936 (vs), 844 (m), 806 (s), 712 (m) cm^{-1}.

Reaction of 8 and 9 with $HBF_4 \cdot Et_2O$. To a solution of 0.2103 g (0.5390 mmol) of **8**/**9** in ethanol and 4 mL of hexane was added 0.2968 g (1.8326 mmol) of $HBF_4 \cdot Et_2O$, and the mixture was stirred for 18 h. After separation of a white precipitate, which according to the $^{31}P\{^1H\}$ NMR data was identified as a mixture of $(Me_3P)_3RhFBF_3$ (**10**), $[(Me_3P)_4Rh]BF_4$ (**11**), and $(Me_3P)_4RhFBF_3$ (**12**), the filtrate was analyzed by GC (10% Carbowax, 20 m over Chromosorb (2 m × $^1/_8$ in.), 50 °C (1 min) to 130 °C at 25°/min, inlet pressure 21 psi of He). The only CO_2-containing species detected was MeCOOEt.

10: $^{31}P\{^1H\}$ NMR (CH_3CN/CD_3CN, −20 °C) δ 14.52 (dt, $^1J_{PRh}$ = 118.0 Hz, $^2J_{PRhP}$ = 32.0 Hz, trans PCH_3), −3.84 (dd, $^1J_{PRh}$ = 88.2 Hz, $^2J_{PRhP}$ = 32.0 Hz, cis PCH_3).

11: $^{31}\{^1H\}$ NMR (CH_3CN/CD_3CN, −20 °C) δ −5.97 (d, $^1J_{PRh}$ = 88.1 Hz).

12: $^{31}P\{^1H\}$ NMR (CH_3CN/CD_3CN, −20 °C) δ −7.41 (dd, $^1J_{PRh}$ = 85.1 Hz, $^2J_{PRhP}$ = 23.6 Hz), −7.80 (dd, $^1J_{PRh}$ = 85.9 Hz, $^2J_{PRhP}$ = 23.3 Hz).

Reaction of 3 with Ag[O_2CPh]. To a suspension of 0.4135 g (0.9341 mmol)/0.4335 g (0.9793 mmol) of **3** in 10 mL of toluene/8 mL of THF cooled to −60 °C was added 0.2567 g (1.1209 mmol)/0.2691 g (1.1751 mmol) of Ag[O_2CPh]. While warming, the reaction mixture darkened, and a metallic silver coat appeared on the glass flask. After separation of a black precipitate (after 17 h for the toluene medium/3 h for the THF medium), the yellow filtrate was concentrated to dryness. ^1H NMR and IR spectra revealed the same absorptions independent of the reaction procedure. In contrast to **5** and **6**, this product was unaffected by vacuum: ^1H NMR (C_6D_6) δ 8.70 (m), 7.20 (m), 1.60–0.95 (m); IR (C_6H_6) $\nu(OCO)_{as}$ 1620 (m, sh), 1610 (s), $\nu(OCO)_s$ 1352 (vs), ν(C- -C) 1570 (m), $\delta(CH_3)$ 1416 (w), $\delta_s(CH_3P)$ 1296 (m), 1285 (m), $\rho(CH_3P)$ 947 (s) cm^{-1}.

(η^1-Acetato)carbonylbis(triphenylphosphine)rhodium (14). A solution of 0.2540 g (0.3788 mmol) of $(Ph_3P)_2$(CO)Rh–Me (**13**) was pressurized with 200 psi of CO_2 for 69 h. An orange precipitate, mainly $[Rh(PPh_3)_2(\mu\text{-}CO)(THF)]_2$ (**15**), was separated. The filtrate was evaporated to dryness, and IR and ^1H NMR spectroscopic investigations of the remaining orange residue revealed the presence of **14**, as well as **13**, **15**, and other metal carbonyls (ν(CO) 2005, 1932 cm^{-1}). At pressures of 50 and 100 psi no reaction of CO_2 with **13** was detectable within 8 h.

Reaction of $(Ph_3P)_2$(CO)Ir–Me (16) with CO_2. A solution of 0.2865 g (0.3770 mmol) of $(Ph_3P)_2$(CO)Ir–Me in 25 mL of THF was pressurized with 200 psi of CO_2 for 5 days. IR monitoring showed formation of four new metal carbonyl species (ν(CO) 2006.7, 1969.6, 1936.8, 1919.4 cm^{-1} in the ratio 1.0:2.2:1.3:4.1), but no indication of the formation of a uni- or bidentate acetato ligand. Separation of the four compounds by crystallization or thin-layer chromatography was not achieved.

Crystallographic Studies

Crystal data and parameters for the collection and refinement of data are contained in Table I. A crystal of **4** was attached to a fine glass fiber with epoxy cement. Preliminary photographic evidence showed $2/m$ Laue symmetry; on the basis of systematic absences, **4** was determined to crystallize in $P2_1/n$. Unit cell dimensions were derived from the least-squares fit of the angular settings of 25 reflections with 20° < 2θ < 30°. Correction for absorption was not needed (μ = 10.5 cm^{-1}, regular crystal shape, <10% variation in ψ scans). A profile-fitting procedure

Table I. Crystal, Data Collection, and Refinement Parameters for 4

formula	$C_{15}H_{32}P_3Rh^I$
space group	$P2_1/n$
a, Å	9.733 (4)
b, Å	17.488 (6)
c, Å	12.021 (5)
β, deg	99.66 (4)
V, Å^3	2017 (1)
Z	4
cryst size, mm	0.20 × 0.22 × 0.40
cryst color	orange
μ, cm^{-1}	10.5
ρ(calcd), g cm^{-3}	1.34
temp, °C	23
diffractometer	Nicolet R3m/μ
radiation	Mo Kα
wavelength, Å	0.71073
scan method	ω
2θ scan range, deg	$4 \leq 2\theta \leq 50$
scan speed, deg min^{-1}	5–20 (variable)
no. of rflns collcd	3874
no. of indpndt rflns	3555
R(int), %	1.91
no. of indpndt rflns, $F_o > 5\sigma(F_o)$	2895
std rflns	3 std/197 rflns
R_F,[a] %	2.99
R_{wF},[a] %	3.67
g	0.001
GOF[b]	1.174
Δ/σ	0.005
$\Delta\rho$(max), e Å^{-3}	0.35

[a] $R_F = \sum|\Delta|/\sum|F_o|$ and $R_{wF} = \sum(|\Delta|w^{1/2})/\sum(|F_o|w^{1/2})$, where $\Delta = |F_o| - |F_c|$. [b] $GOF = [\sum w(\Delta^2)/N_{observns} - N_{params})]^{1/2}$.

---

[11] (a) Bennett, M. A.; Longstaff, P. A. *Chem. Ind.* (*London*) **1965**, 846. (b) Young, J. F.; Osborn, J. A.; Jardine, F. H.; Wilkinson, G. *J. Chem. Soc., Chem. Commun.* **1965**, 131. (c) Vaska, L.; Rhodes, R. E. *J. Am. Chem. Soc.* **1965**, *87*, 4970.

[12] Osborne, J. A.; Jardine, F. H.; Young, J. F.; Wilkinson, G. *J. Chem. Soc.* **1966**, 1711.

Table II. Atomic Coordinates ($\times 10^4$) and Isotropic Thermal Parameters ($Å^2 \times 10^3$) for $C_{15}H_{32}P_3Rh^1$

	x	*y*	*z*	U^a
Rh	1339.9 (3)	1229.0 (2)	1685.5 (2)	34.8 (1)
P(1)	2818 (1)	1978.2 (6)	860.4 (9)	44.8 (3)
P(2)	3059 (1)	417.9 (6)	2542.2 (9)	44.0 (3)
P(3)	−463 (1)	508.0 (6)	2108.7 (9)	45.4 (3)
C(1)	−474 (5)	2595 (3)	1964 (4)	56 (2)
C(2)	−1517 (5)	3145 (3)	1727 (5)	70 (2)
C(3)	−2333 (5)	3167 (3)	669 (5)	70 (2)
C(4)	−2086 (5)	2669 (3)	−139 (4)	64 (2)
C(5)	−1020 (4)	2118 (3)	101 (4)	51 (1)
C(6)	−175 (4)	2055 (2)	1184 (3)	42 (1)
C(7)	2079 (5)	2580 (3)	−326 (5)	76 (2)
C(8)	3815 (7)	2703 (3)	1761 (6)	91 (3)
C(9)	4181 (5)	1504 (3)	203 (4)	68 (2)
C(10)	4717 (5)	852 (3)	3196 (4)	68 (2)
C(11)	3686 (6)	−365 (3)	1730 (5)	85 (2)
C(12)	2797 (6)	−118 (3)	3799 (4)	75 (2)
C(13)	−461 (6)	−511 (3)	1749 (5)	78 (2)
C(14)	−773 (7)	495 (4)	3573 (5)	93 (3)
C(15)	−2243 (5)	736 (4)	1434 (6)	98 (3)

[a] Equivalent isotropic *U* defined as one-third of the trace of the orthogonalized U_{ij} tensor.

Table III. Bond Lengths and Angles for $C_{15}H_{32}P_3Rh^1$

	(a) Bond Lengths (Å)		
Rh-P(1)	2.291 (1)	P(3)-C(13)	1.833 (5)
Rh-P(2)	2.301 (1)	P(3)-C(14)	1.836 (6)
Rh-P(3)	2.286 (1)	P(3)-C(15)	1.830 (5)
Rh-C(6)	2.079 (4)	C(1)-C(2)	1.393 (7)
P(1)-C(7)	1.821 (6)	C(1)-C(6)	1.396 (6)
P(1)-C(8)	1.835 (6)	C(2)-C(3)	1.383 (7)
P(1)-C(9)	1.850 (6)	C(3)-C(4)	1.355 (8)
P(2)-C(10)	1.836 (5)	C(4)-C(5)	1.410 (6)
P(2)-C(11)	1.843 (6)	C(5)-C(6)	1.423 (5)
P(2)-C(12)	1.832 (6)		
	(b) Bond Angles (deg)		
P(1)-Rh-P(2)	94.8 (1)	C(10)-P(2)-C(12)	95.3 (2)
P(1)-Rh-P(3)	166.6 (1)	C(11)-P(2)-C(12)	99.2 (3)
P(2)-Rh-P(3)	95.0 (1)	Rh-P(3)-C(13)	116.9 (2)
P(1)-Rh-C(6)	86.8 (1)	Rh-P(3)-C(14)	118.5 (2)
P(2)-Rh-C(6)	170.0 (1)	C(13)-P(3)-C(14)	102.7 (3)
P(3)-Rh-C(6)	85.1 (1)	Rh-P(3)-C(15)	119.1 (2)
Rh-P(1)-C(7)	118.4 (2)	C(13)-P(3)-C(15)	98.4 (3)
Rh-P(1)-C(8)	116.6 (2)	C(14)-P(3)-C(15)	97.6 (3)
C(7)-P(1)-C(8)	99.4 (3)	C(2)-C(1)-C(6)	123.9 (4)
Rh-P(1)-C(9)	118.4 (2)	C(1)-C(2)-C(3)	119.5 (5)
C(7)-P(1)-C(9)	98.1 (2)	C(2)-C(3)-C(4)	119.9 (5)
C(8)-P(1)-C(9)	102.5 (3)	C(3)-C(4)-C(5)	120.4 (4)
Rh-P(2)-C(10)	117.2 (2)	C(4)-C(5)-C(6)	122.2 (4)
Rh-P(2)-C(11)	120.1 (2)	Rh-C(6)-C(1)	119.5 (3)
C(10)-P(2)-C(11)	100.9 (3)	Rh-C(6)-C(5)	126.3 (3)
Rh-P(2)-C(12)	119.6 (2)	C(1)-C(6)-C(5)	114.1 (4)

was applied to all intensity data to improve the precision of weak reflections. The data were corrected for secondary extinction effects.

The structure of **4** was solved via heavy-atom methods, locating the Rh atom. The remaining non-hydrogen atoms were found in subsequent difference Fourier syntheses and were refined anisotropically. Idealized hydrogen atom positions were calculated [d(C–H) = 0.96 Å; thermal parameters equal 1.2 times the isotropic equivalent for the carbon to which it was attached]. **4** crystallizes with one molecule of $C_{15}H_{32}P_3Rh$ per asymmetric unit.

An inspection of F_o vs F_c values and trends based on sin θ, Miller index, or parity group showed no systematic errors in the data. All computer programs used in the data collection and refinements are contained in the Nicolet program packages P3, SHELXTL (version 5.1), and XP (Nicolet XRD, Madison, WI). Atomic coordinates are provided in Table II; bond distances and angles, in Table III. Additional crystallographic data are available as supplementary material.

Results and Discussion

Tris(triphenylphosphine)phenylrhodium(I) has been reported to undergo an insertion reaction with carbon dioxide to afford the benzoate derivative (eq 3).[13] The reaction product (**2**) was fully characterized by NMR and IR spectroscopy, and X-ray structural analysis. We have repeated this reaction and have found that under 300 psi of CO_2, **2** is the sole reaction product.

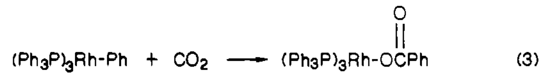

$$(Ph_3P)_3Rh\text{-}Ph + CO_2 \longrightarrow (Ph_3P)_3Rh\text{-}OC(=O)Ph \quad (3)$$

1 **2**

In an effort to explore the generality of this reaction, as well as how the nature of the ancillary phosphine ligands and the Rh–C bond influences its course, we have examined other $(R_3P)_3RhR'$ complexes' reactivity toward carbon dioxide. The $(Me_3P)_3Rh$–Ph derivative was prepared by an alternative route to that previously described in the literature.[14] Reaction of PhLi with $[Me_3P)_4Rh]Cl$ at −10 °C afforded $(Me_3P)_3Rh$–Ph in 74% purified yield (eq 4).

$$[(Me_3P)_4Rh]Cl + PhLi \xrightarrow{-10\ °C} (Me_3P)_3Rh\text{–}Ph + LiCl + Me_3P \quad (4)$$

$(Me_3P)_3Rh$–Ph was obtained as a yellow crystalline product, and its solid-state structure was determined by X-ray crystallography. A view of the molecule is depicted in Figure 1, where the atomic numbering scheme is defined as well.

The molecular geometry of **4** is that of a slightly distorted square-planar complex. The mean deviation from the least-squares plane defined by the four ligands, which contains the rhodium atom, is 0.19 Å. The two mutually trans phosphines (P(1) and P(3)) lie below the plane by 0.19 Å with a P(1)–Rh–P(3) bond angle of 166.6°, whereas the carbon of the phenyl ligand (C(6)) and the trans phosphine group (P(2)) are 0.22 and 0.16 Å above the plane with a C(6)–Rh–P(2) bond angle of 170.0°. the phenyl group, located 2.079 (4) Å from the metal center, is perpendicular to the square plane formed by the four ligands bound to rhodium. The Rh–P bond distance opposite the phenyl group is 2.301 (1) Å, with the two mutually trans Rh–P distances being 2.291 (1) and 2.286 (1) Å. Hence, the phenyl ligand does not impart a trans influence in this square-planar complex.

Species **4** is considerably more reactive toward carbon dioxide than its triphenylphosphine analogue (**1**). For example, the reaction of **1** with CO_2 at 300 psi requires about 24 h to go to completion, whereas the reaction of **4** with CO_2 at 150 psi is complete within 3 h. Upon careful monitoring of the appearance of the crucial symmetric and asymmetric carboxylate infrared bands at 1609 and 1431 cm^{-1}, it is clear that formation of **5** is quite CO_2 pressure dependent in the range 30–150 psi. Besides the initially formed monodentate product **5**, a subsequent reaction involving coordination of the acyl oxygen with concomitant displacement of Me_3P affords $(Me_3P)_2Rh(\eta^2\text{-}O_2CPh)$ (**6**) (eq 5).

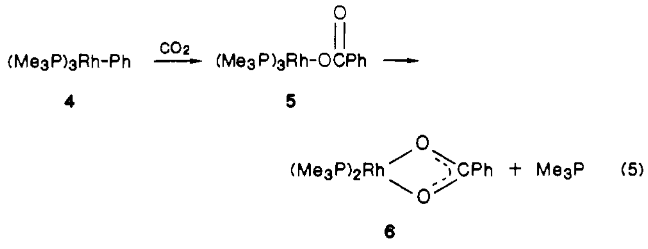

The separation of the infrared symmetric and asymmetric carboxylate bands of **6** of only 47 cm^{-1} (1495 and 1448 cm^{-1}) is indicative of the benzoate ligand binding in a chelating manner as depicted in eq 5. Species **5** was shown to be an intermediate in the production of **6** in that at a CO_2 pressure of 15 psi, where conversion of **4** to **5** is very slow, **5** was observed to afford **6** without a detectable decrease in **4**. By means of high-pressure in situ IR spectroscopy, we were unable to detect an intermediate, i.e., a CO_2–metal adduct, during the formation of **5** from **4** at 150 psi

---

(13) (a) Kolomnikov, I. S.; Gusev, A. O.; Belopotapova, T. S.; Grigoryan, M. Kh.; Lysyak, T. V.; Struchkov, Yu. T.; Volpin, M. E. *J. Organomet. Chem.* **1974**, *69*, C10. (b) Gusev, A. I.; Struchkov, Yu. T. *Zh. Strukt. Khim.* **1974**, *15*, 282; *J. Struct. Chem. (Engl. Transl.)* **1974**, *15*, 256.

(14) Jones, R. A.; Wilkinson, G. *J. Chem. Soc., Dalton Trans.* **1979**, 472.

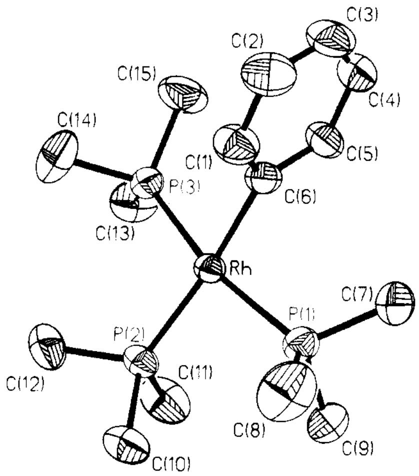

Figure 1. Atom labeling for the $(Me_3P)_3Rh-Ph$ complex.

of CO_2. Because of the deviation from planarity of the four ligands around the rhodium center and the orientation of the phenyl ring (vide supra), steric inhibition toward CO_2 coordination at the metal center prior to structural reorganization is anticipated. That is, an I_a (concerted) reaction pathway is favored over an A process. This steric crowding at the metal center is illustrated in a space-filling model (figure deposited in supplementary material).

In contrast to the stability of the $(Ph_3P)_3RhO_2CPh$ derivative toward decarboxylation, $(Me_3P)_3RhO_2CPh$ is unstable in the absence of a carbon dioxide atmosphere. That is, upon removal of the CO_2 atmosphere during solvent reduction at reduced pressure, reaction 5 reverts to the starting phenyl complex. This is readily seen in the infrared spectrum, where the symmetric and asymmetric $\nu(CO_2)$ bands of **5** disappear immediately upon elimination of CO_2, with the corresponding vibrations in **6** decreasing in intensity at a slower rate. Concomitantly, the proton resonance for the Rh–Ph linkage reappears in the ^1H NMR spectrum. Hence, reaction 5 is represented as an equilibrium process. Presumably, the enhanced stability of the Rh–Ph bond in the Me_3P derivative coupled with the destabilization of the $Rh-O_2CPh$ bond, as compared with the corresponding bonds in the PPh_3 derivative, accounts for the observed thermodynamic behavior.[15,16] Attempts to prepare $(Me_3P)_3RhO_2CPh$ from a metathesis reaction of $[(Me_3P)_4Rh]Cl$ and AgO_2CPh were unsuccessful due to a redox process involving Ag(I) and Rh(I).

The sensitivity of the CO_2 insertion reaction to the nature of the phosphine ligands and the Rh–R bond is further revealed during reactions of $(R_3P)_3Rh-Me$ derivatives with CO_2. Although the review literature[17] reports that the reaction of carbon dioxide with $(Ph_3P)_3Rh-Me$ is completely analogous to that well documented for $(Ph_3P)_3Rh-Ph$, we have been unable after numerous attempts to reproduce those results. During the reaction of $(Ph_3P)_3Rh-Me$ with CO_2 at 70 psi for 17 h, no consistent pattern of η^1- or η^2-acetate bands was observed in the infrared spectrum. Albeit a reaction between 7 and carbon dioxide took place, no definitive information regarding the nature of the products was obtained. After workup of the reaction mixture in chlorinated solvents, $(Ph_3P)_2Rh(CO)Cl$ was isolated as a crystalline product.[18,19]

On the other hand, $(Me_3P)_3Rh-Me$ reacts with CO_2 in a manner similar to that described for species **4**. At atmospheric carbon dioxide pressure the insertion reaction (6) proceeds slowly

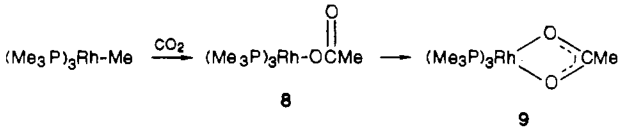

(6)

at ambient temperature, requiring 1 week to go to completion. The infrared spectrum unambiguously reveals initial formation of the η^1-acetate species **8** ($\Delta\nu(CO_2) = 252\ cm^{-1}$), which subsequently rearranges to **9** ($\Delta\nu(CO_2) = 29\ cm^{-1}$). In further support of reaction 6, addition of $HBF_4 \cdot Et_2O$ in ethanol affords $MeCO_2Et$ as the only CO_2-containing species. Hence, MeCOOH must be the only initially formed cleavage product.

Replacement of a basic triphenylphosphine ligand in $(Ph_3P)_3Rh-Me$ with carbon monoxide, forming species **13**, leads to a decrease in electron density at the rhodium center. **13** reacts slowly with 200 psi of CO_2 to afford the insertion product **14** ($t_{1/2} = 70$ h). Because of the prolonged reaction time, considerable decomposition of **13** to **15** occurs. This decomposition reaction

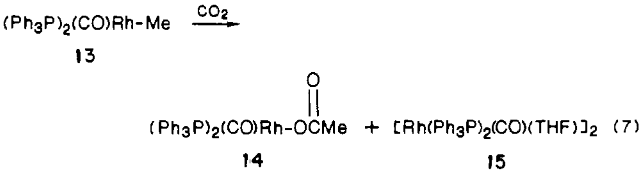

(7)

has been previously reported in polar solvents.[20] Species **15** was also identified by conversion to $[Rh(Ph_3P)_2(CO)(CH_2Cl_2)]_2$.[21] The analogous iridium complex, $(Ph_3P)_2(CO)Ir-Me$, where a stronger IR–Me bond is present, was unreactive toward carbon dioxide.

Conclusions

The results reported herein on square-planar rhodium complexes, $(R_3P)_3RhR'$, are consistent with those we have previously observed for CO_2 insertion processes involving anionic group 6 metal carbonyl derivatives. Upon an increase in the electron density at the metal center, the carbon dioxide insertion reaction proceeds at a faster rate. This was achieved either by decreasing the electron-withdrawing character of the R′ ligand (R′ = Me faster than R′ = Ph) or by increasing the basicity of the phosphine ligands ($PMe_3 > PPh_3 > CO$). A caveat that must be reiterated here is that these electronic effects will be expected to dominate in the *absence* of steric congestion about the metal–carbon center. Steric effects may be particularly important in these instances where several phosphine ligands are involved. These findings, coupled with the CO_2 pressure dependence, lead us to suggest a concerted I_a mechanism for CO_2 insertion reactions involving square-planar metal substrates. An intermediate analogous to that shown in structure A would be appropriate.

Acknowledgment. The financial support of this research by the National Science Foundation (Grant CHE 86-03681) is greatly appreciated. G.G. was recipient of a DAAD/NATO Scholarship, for which we are most grateful.

Supplementary Material Available: Anisotropic thermal parameters (Table 1S), hydrogen atom coordinates (Table 2S), and a space-filling diagram of $(Me_3P)_3Rh-Ph$ (3 pages); a listing of observed and calculated structure factors (Table 3S) (17 pages). Ordering information is given on any current masthead page.

---

(15) The metal–carbon bond is expected to be stabilized upon addition of electron-donating ligand to the metal center; i.e., replacement of Ph_3P by Me_3P should result in a stronger Rh–Ph bond.[16]

(16) Darensbourg, D. J.; Bauch, C. G.; Rheingold, A. L. *Inorg. Chem.* **1987**, *26*, 977.

(17) (a) Volpin, M. E.; Kolomnikov, I. S. *Organomet. React.* **1975**, *5*, 313; *Pure Appl. Chem.* **1973**, *33*, 567. (b) Kolomnikov, I. S.; Grigoryan, M. Kh. *Russ. Chem. Rev.* (*Engl. Transl.*) **1978**, *47*, 334.

(18) An X-ray structure of this complex has been completed: Rheingold, A. L.; Geib, S. J. *Acta Crystallogr., Sect. C: Cryst. Struct. Commun.* **1987**, *C43*, 784. The structure (monoclinic $P2_1/n$) is similar to that previously reported as a noncentrosymmetric triclinic polymorph with "implausible" bond lengths.[19]

(19) Del Pra, A.; Zanotti, G.; Segala, P. *Cryst. Struct. Commun.* **1979**, *8*, 959.

(20) Evans, D.; Yagupsky, G.; Wilkinson, G. *J. Chem. Soc. A* **1968**, 2660.

(21) Dammann, C. B.; Singlh, P.; Hodgson, D. J. *J. Chem. Soc., Chem. Commun.* **1972**, 586; *Inorg. Chem.* **1973**, *12*, 1335.